Rotationally resolved vibronic spectra of the van der Waals modes of benzene–Ar and benzene–Kr complexes

E. Riedle
Max-Born-Institut für Nichtlineare Optik und Kurzzeitspektroskopie, Rudower Chaussee 6, D-12489 Berlin, Germany

R. Sussmann,[a] Th. Weber,[b] and H. J. Neusser
Institut für Physikalische und Theoretische Chemie, Technische Universität München, Lichtenbergstrasse 4, D-85748 Garching, Germany

(Received 5 January 1995; accepted 27 September 1995)

Rotationally resolved vibronic spectra of eight van der Waals bands built onto the 6_0^1 transition of the bare molecule are reported for the complexes $C_6H_6 \cdot Ar$, $C_6D_6 \cdot Ar$, and $C_6H_6 \cdot {}^{84}Kr$. The rotational structure of most of the bands is identified as that of a perpendicular transition with Coriolis coupling constants nearly the same as those of the 6_0^1 band of the respective complex. We therefore conclude that the excited van der Waals modes of the three complexes have a_1 symmetry. Precise rotational constants are fitted to the large number of unblended lines assigned in each spectrum. In contrast, the lowest energy van der Waals bands of both $C_6H_6 \cdot Ar$ and $C_6D_6 \cdot Ar$ display a completely different rotational structure which can neither be explained by a genuine perpendicular nor a genuine parallel transition. This situation will be analyzed in detail in accompanying work and the final vibronic assignments deduced. The rovibronic lines in all the spectra show a linewidth of 130 MHz that is solely due to the laser linewidth and to residual Doppler broadening in the molecular jet. It is concluded that the excited vibronic combination states of intramolecular and van der Waals vibrations do not predissociate on the nanosecond time scale of our experiment. Two of the reported spectra show irregularities in the rotational structure that are explained by coupling to adjacent combination states. © *1996 American Institute of Physics.* [S0021-9606(96)02001-5]

I. INTRODUCTION

One of the most important goals in the study of molecular clusters is the determination of the van der Waals potential between the weakly bound atom or molecule and the substrate to which it is attached. Of all known techniques, high resolution spectroscopy can perform this task with greatest precision. In principle, direct transitions to the rovibrational eigenstates of the van der Waals potential can be observed in the far IR. However, until now such studies have only been performed for very select small molecules. More conveniently, van der Waals excitation is observed in combination with either vibrational or electronic excitation. Particularly clusters containing organic molecules can best be investigated in the UV range of the spectrum. Even under moderate resolution ($\Delta\nu \leqslant 1\ cm^{-1}$), a well-resolved vibronic structure is observed close to the band assigned as the intramolecular transition and interpreted as additional excitation of van der Waals modes. A large number of recent reports have focused on this topic.[1–18]

In these experiments the assignment of the various bands has mostly been based on the comparison of the observed and calculated energies and consideration of selection rules thought to be valid for the system under investigation. Discrepancies between observed and calculated frequencies are then removed by an ''improved'' model potential. Due to the limited spectral resolution of most studies, no use can be made of the additional information contained in the rotational structure of the spectra. This information includes the connection between the band type and the symmetry of the excited vibronic state and the magnitudes of the rotational constants for the various intermolecular vibrational states.

Initially, empirical atom–atom pairwise potentials were used in the calculations. Only recently have *ab initio* studies for some organic molecule–rare gas clusters been reported.[19–21] One dimensional cuts through these potentials were then used to calculate nearly harmonic normal mode energies.[2,6,8,22] At best, the stretch–bend coupling due to Fermi resonance between the fundamental of the stretch and the overtone of the bend was taken into consideration.[5] However, full 3D calculations that are now available for a number of systems[11,12,15,17,23–28] show that this simplification is certainly not as often permissible as for chemically bound systems. In the 3D calculations, benzene–Ar developed into a prototype test case owing to its high symmetry and relative simplicity. But even the 3D calculations do not predict the intensities of transitions correctly and therefore a considerable amount of ''intuition'' is still needed to compare experiment and theory. Since only very few van der Waals bands can be observed for a given complex, ambiguities remain.

We show in this work that decisive new information can be obtained from the rotational structure and the determina-

[a]Present address: Fraunhofer Institut für Atmosphärische Umweltforschung, Kreuzeckbahnstr. 19, D-82467 Garmisch-Partenkirchen, Germany.
[b]Present address: Technolas Umwelt- und Industrieanalytik GmbH, Lochhamer Schlag 19, D-82166 Gräfelfing, Germany.

tion of rotational constants for all observable states. The recording of rotationally resolved electronic spectra of clusters of organic molecules is not possible with standard molecular beams and lasers. However, in a number of contributions,[1,12,29–31] in particular from this laboratory,[32–41] it was shown that this is nevertheless possible with improved experimental techniques. We now extend this work to the van der Waals bands observed in the vicinity of the 6_0^1 band of three benzene–rare gas complexes. Three new spectra are reported and analyzed for $C_6H_6 \cdot Ar$, three for $C_6D_6 \cdot Ar$, and two for $C_6H_6 \cdot {}^{84}Kr$. It is found that in all spectra many unblended rovibronic lines can be found and used for the unambiguous determination of the rotational constants. The spectroscopic situation in these complexes is somewhat more complicated than in the case of *p*-difluorobenzene–Ar (*p*-DFB–Ar), considered in parallel work.[39,41] This is because the bending mode is degenerate in benzene–rare gas complexes and complications can arise due to Coriolis coupling. In *p*-DFB–Ar the lowest van der Waals band was observed at nearly the same frequency as in benzene–Ar. It was assigned as a transition to the first quantum of the short in-plane bending vibration by analysis of the well-resolved rotational contour. The appearance of the band was attributed to Herzberg–Teller activity of the intermolecular mode.[39] Valuable additional information was obtained from an unprecedented number of bands observed up to 125 cm^{-1} of intermolecular energy.[41]

The experimental setup used to record the rotationally resolved spectra is briefly reviewed in Sec. II. In Sec. III A the low resolution overview spectra of the three clusters under investigation are discussed. The rotational structure of perpendicular vibronic bands of benzene–rare gas clusters is then explained in Sec. III B. This sets the stage for the detailed spectroscopic analysis of the newly reported van der Waals vibronic bands of $C_6H_6 \cdot Ar$ (Sec. III C), $C_6H_6 \cdot {}^{84}Kr$ (Sec. III D) and $C_6D_6 \cdot Ar$ (Sec. III E). Finally, the implications for vibrational dissociation of the clusters are discussed in Sec. IV together with the information on the vibronic assignment that can be deduced from the rotational analysis. The successful rotational analysis of the lowest energy van der Waals bands of both $C_6H_6 \cdot Ar$ and $C_6D_6 \cdot Ar$ will be presented in the accompanying paper[42] together with the final vibronic assignments and calculations that explain the observed spectra very well.

II. EXPERIMENT

The experimental setup used in this work is similar to the one used previously to record rotationally resolved spectra of the benzene–noble gas dimers[32–35,37] and trimers.[36] Only a brief review will be given here, with particular emphasis on the experimental conditions of the new measurements presented in this work.

The benzene–Ar clusters were formed in a skimmed supersonic jet expansion of a premixed gas sample of 40 mbar benzene and 5 bar argon. The Ar pressure in the present study was chosen somewhat higher than in the previously reported study of the 6_0^1 bands and resulted in a reduced rotational temperature of 1.5–2.0 K. For the benzene–Kr study a gas sample of 6 mbar benzene and 4 bar krypton in natural isotopic mixture was used. Due to the mass selectivity of the ion detection technique the vibronic spectra of the most abundant benzene–^{84}Kr (57%) were measured in isolation from the other isotopic clusters.[33] The collimation of the molecular beam (50:1) leads to a residual Doppler broadening of about 40 MHz at a typical transition frequency of around 38 600 cm^{-1}.

The pulsed-amplified and frequency-doubled light of a single-mode cw dye laser excites the clusters to the desired vibrational level in the S_1 electronic state. Owing to the narrow-band Fourier-transform-limited UV pulses ($\Delta\nu_{UV} \sim 120$ MHz), rotational resolution is achieved in the vibronic spectra. After a small time delay of 2–5 ns after excitation, a second UV-pulse from a frequency-doubled pulsed dye laser ionizes the excited clusters, leading to an excess energy of about 700 cm^{-1} above the ionization threshold. The frequency of the ionization laser is carefully chosen to not create any additional $S_1 \leftarrow S_0$ excitation of the clusters. Both laser intensities are controlled by attenuation and defocusing to avoid saturation broadening and distortion of the rotational structure due to selective saturation of those rovibronic transitions that have large Hönl–London factors, as previously observed for the bare benzene molecule.[43] During the experiments, pulse energies of 0.1–1 mJ/cm^2 in 5 ns were used for excitation at the interaction zone and 20 mJ/cm^2 in 10 ns for ionization.

Overview spectra with a resolution of 0.5 cm^{-1} were measured in a *one*-color REMPI experiment with the pulsed dye laser alone. The ions were detected mass-selectively in a modified Wiley–McLaren-type time-of-flight mass spectrometer[44] with a resolution of $m/\Delta m \sim 200$. To increase the sensitivity of the detection system, which may be partly saturated by the large number of $C_6H_6^+$ ions arriving earlier than the complex ions, we placed an additional grid in front of the detector. A potential comparable to the accelerating voltage was applied to repel the unwanted ions and was switched off shortly before the cluster ions under investigation arrived at the grid.

III. EXPERIMENTAL RESULTS

A. Overview spectra in the vicinity of the 6_0^1 band of benzene–noble gas clusters

The pure $S_1 \leftarrow S_0$ electronic transition has neither been observed for the benzene molecule nor its noble gas heterodimer clusters. For benzene, it is well established that this is due to the high symmetry of the molecule (D_{6h}) and the symmetry of the S_1 state (B_{2u}) that make the $S_1 \leftarrow S_0$ transition symmetry forbidden.[45] For $C_6H_6 \cdot Ar$, both early[2,46] and very recent investigations[47] have very carefully searched for the origin transition and found an upper limit for the intensity of the origin transition as compared to the intensity of the 6_0^1 transition of 0.1%. Instead of the pure electronic transition, the Herzberg–Teller allowed 6_0^1 band is found as a false origin in the one-photon absorption and excitation spec-

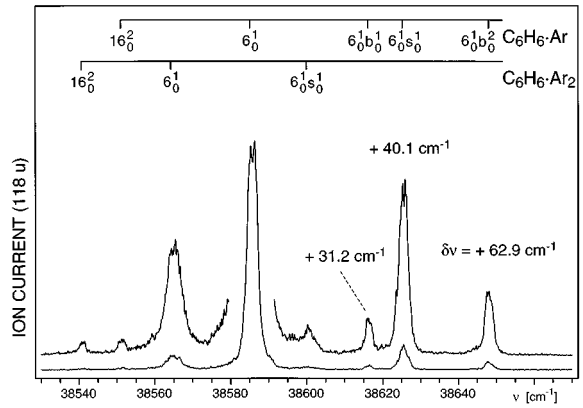

FIG. 1. Low resolution spectrum in the region of the 6_0^1 band of the $C_6H_6{\cdot}Ar$ cluster for two laser intensities, monitored by the ion current at the $C_6H_6{\cdot}Ar$ mass (118 u). Three of the seven peaks seen in addition to the 6_0^1 band are due to transitions in $C_6H_6{\cdot}Ar_2$ as indicated at the top and discussed in the text. The three bands of $C_6H_6{\cdot}Ar$ at $\delta\nu=+31.2$, 40.1, and 62.9 cm^{-1} are due to the excitation of van der Waals modes in addition to the fundamental excitation in the benzene part of the cluster. Rotationally resolved spectra of these bands are presented and analyzed in this work.

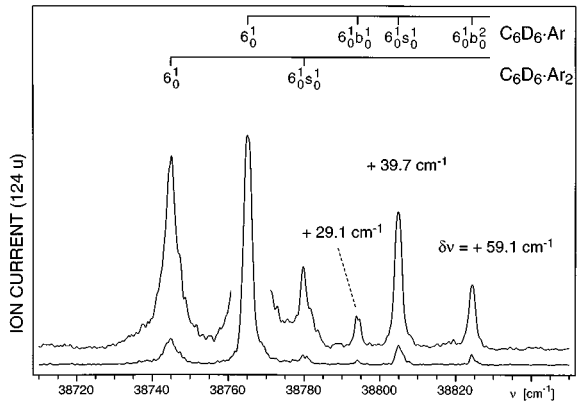

FIG. 2. Low resolution spectrum in the region of the 6_0^1 band of the $C_6D_6{\cdot}Ar$ cluster for two laser intensities, monitored by the ion current at the $C_6D_6{\cdot}Ar$ mass (124 u). Two of the five peaks seen in addition to the 6_0^1 band are due to transitions in $C_6D_6{\cdot}Ar_2$ as indicated at the top and discussed in the text. The three bands of $C_6H_6{\cdot}Ar$ at $\delta\nu=+29.1$, 39.7, and 59.1 cm^{-1} are due to the excitation of van der Waals modes in addition to the fundamental excitation in the benzene part of the cluster. Rotationally resolved spectra of these bands are presented and analyzed in this work.

trum. The observation of simultaneous van der Waals mode excitation is therefore best possible in the vicinity of the 6_0^1 band. This is indeed the spectral range observed in previous low resolution studies. In order to identify observable combination bands containing van der Waals excitation, low resolution overview spectra of the various clusters under investigation were recorded.

Figure 1 displays the electronic spectrum of $C_6H_6{\cdot}Ar$ between 38 530 cm^{-1} and 38 670 cm^{-1} at a resolution of 0.5 cm^{-1}. Both traces were measured by monitoring the ion current at 118 u, i.e., the mass of $C_6H_6{\cdot}Ar$. For increased sensitivity, a higher laser intensity was used for the upper recording. The strongest transition found is the 6_0^1 band with a red shift of 21.0 cm^{-1} from the 6_0^1 band of C_6H_6.[2,32,46] In a recent publication from this laboratory it was shown that three of the seven bands found in the vicinity of the 6_0^1 band are indeed not due to vibronic bands of $C_6H_6{\cdot}Ar$ but instead are due to bands of $C_6H_6{\cdot}Ar_2$.[36] This was proven by a careful analysis of the rotationally resolved spectra of these bands. $C_6H_6{\cdot}Ar_2$ clusters are initially excited; however, $C_6H_6{\cdot}Ar^+$ ions are eventually detected due to a fast dissociation of the excited $C_6H_6{\cdot}Ar_2$ clusters. In addition, the band at 38 551 cm^{-1} was identified as the 16_0^2 transition of $C_6H_6{\cdot}Ar$;[34] i.e., a completely separate vibronic transition and not one of the combination bands of interest at present. All of these previous assignments are summarized at the top of Fig. 1.

The rotationally resolved spectra of the three remaining bands at $\delta\nu=+31.2$, $+40.1$, and $+62.9$ cm^{-1} relative to the 6_0^1 band will be presented and discussed in this paper. It will be shown that they indeed belong to $C_6H_6{\cdot}Ar$ and that their rotational analysis can unambiguously determine the vibronic assignment.

The corresponding low resolution spectrum of $C_6D_6{\cdot}Ar$ is shown in Fig. 2. The strongest transition found is the 6_0^1 band with a red shift of 20.8 cm^{-1} from the 6_0^1 band of C_6D_6.[32] Again, two of the five extra features observed are attributed to $C_6D_6{\cdot}Ar_2$ according to rotational analyses of their high resolution spectra. The 16_0^2 transitions found for $C_6H_6{\cdot}Ar$ and $C_6H_6{\cdot}Ar_2$ are not found in this spectral region for the deuterated species since ν_{16} and ν_6 have a considerably different isotope shift. For the remaining three bands at $\delta\nu=+29.1$, $+39.7$, and 59.1 cm^{-1}, rotationally resolved spectra will be presented and discussed below. The relative heights of the bands are similar to those found in $C_6H_6{\cdot}Ar$. Each peak is shifted slightly towards the 6_0^1 band, as would be expected under the assumption of identical vibrational assignments and the typical isotope shift of vibrations upon deuteration.

The overview spectrum of $C_6H_6{\cdot}^{84}Kr$ shown in Fig. 3 displays a much simpler structure than that found for

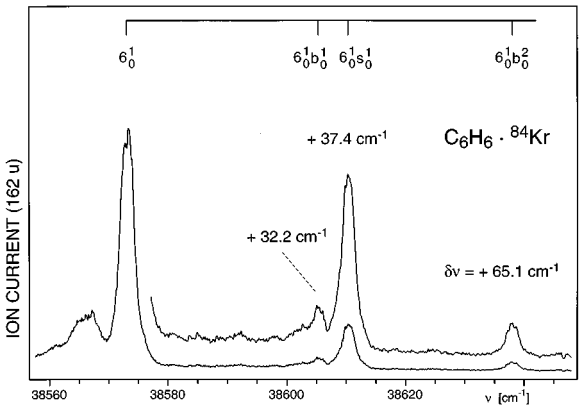

FIG. 3. Low resolution spectrum in the region of the 6_0^1 band of the $C_6H_6{\cdot}^{84}Kr$ cluster for two laser intensities, monitored by the ion current at the $C_6H_6{\cdot}Ar$ mass (162 u). The three bands at $\delta\nu=+32.2$, 37.4, and 65.1 cm^{-1} are due to the excitation of van der Waals modes in addition to the fundamental excitation in the benzene part of the cluster. Rotationally resolved spectra of the two higher energy bands are presented and analyzed in this work.

TABLE I. Spectroscopic constants used for the fitting of the various vibronic bands of C_6H_6–rare clusters. The ground state rotational constants B'' and the centrifugal distortion constants D''_J and D''_{JK} were taken from the relevant microwave work. D''_K cannot be determined from microwave spectra and was constrained to zero. In the same fashion microwave spectra cannot be used to determine A''_0 and this constant was therefore fixed to the value of C''_0 for benzene. For details see text. Since the electronic spectra reported are not precise enough for the determination of S_1 state centrifugal distortion constants, those constants were constrained to the ground state values.

	$C_6H_6\cdot Ar$[a]	$C_6H_6\cdot{}^{84}Kr$[b]	$C_6D_6\cdot Ar$[a]
A''_0 (cm^{-1})	0.094 880 9	0.094 880 9	0.078 509 5
B''_0 (cm^{-1})	0.039 402 58	0.026 541 10	0.037 107 04
$D''_J = D'_J$ (cm^{-1})	1.0867×10^{-7}	0.4386×10^{-7}	0.8916×10^{-7}
$D''_{JK} = D'_{JK}$ (cm^{-1})	$5.9378\ 10^{-7}$	2.6335×10^{-7}	4.8467×10^{-7}
$D''_K = D'_K$ (cm^{-1})	0.000	0.000	0.000

[a]Taken from Ref. 48.
[b]Taken from Ref. 49.

benzene–Ar owing to the lack of contributions from $C_6H_6\cdot{}^{84}Kr_2$. The strongest transition found is the 6_0^1 band with a red shift of 33.4 cm^{-1} from the 6_0^1 band of C_6H_6.[33] Rotationally resolved spectra of the bands at $\delta\nu = +37.4$ and $+65.1$ cm^{-1} will be presented and discussed here. The band at $+32.2$ cm^{-1} was too weak to be recorded at high resolution.

B. The rotational structure of perpendicular vibronic bands of $C_6H_6\cdot Ar$

In the one-photon electronic spectrum of benzene exclusively perpendicular bands have been found.[45] They correspond to transitions to degenerate vibrational states of e_{2g} symmetry in the $^1B_{2u}$ electronic state. Similarly, the previously analyzed bands of $C_6H_6\cdot Ar$ (Refs. 32, 34) were also found to be perpendicular transitions. In a degenerate vibronic state of the prolate symmetric top $C_6H_6\cdot Ar$, the energy $E_{\rm rot}$ of a rotational state $|J,K\rangle$ is given to the precision needed in this work by

$$E_{\rm rot} = B_v J(J+1) + (A_v - B_v)K^2 \mp 2A_v\zeta_{\rm eff}K - D_J J^2(J+1)^2 - D_{JK}J(J+1)K^2 - D_K K^4. \quad (1)$$

Here, A_v and B_v are the rotational constants of the vibronic state and the D's are the centrifugal distortion constants. The term $\mp 2A_v\zeta_{\rm eff}K$ describes the Coriolis splitting of the $(+l)$ and $(-l)$ vibrational angular momentum substates of the degenerate vibronic state. This term vanishes for nondegenerate vibronic states like the pure electronic ground state.

Values of the ground state rotational constants B''_0 of $C_6H_6\cdot Ar$, $C_6D_6\cdot Ar$,[32] and $C_6H_6\cdot{}^{84}Kr$ (Ref. 33) were first determined from the rotationally resolved UV spectra. Subsequently, more precise values of B''_0 (and also values for D''_J and D''_{JK}) were determined from microwave spectra.[48,49] Summarized in Table I, all of these constants were constrained in the interpretation of the electronic spectra presented in this work. To verify the identity of the complexes, a value of B''_0 was fitted to each spectrum in an initial fitting run. In all cases this value agreed with the microwave one to within experimental precision. D''_K cannot be determined from the microwave spectra and it was therefore set to zero. The various centrifugal distortion terms in Eq. (1) typically amount to a few tens of MHz. Accurate values of the distortion constants for the S_1 state cannot be determined from the presently available electronic spectra. Hence, these were also constrained to their ground state values.

Both the microwave spectra[48,49] and the rotationally resolved UV spectra analyzed previously[32–37] and in this work show no sign of asymmetry splitting of individual rovibronic lines. Such a splitting should be particularly large and easily observed for lines with either $K'=1$ or $K''=1$ and large J.[32] It is therefore concluded that the complexes discussed in this work are symmetric tops with $B=C$ in both electronic states. The selection rules obeyed in the microwave spectra preclude the determination of A''_0. This is also true for parallel electronic transitions. For perpendicular ones the upper state is degenerate and split by Coriolis coupling. Of the three constants A''_0, A'_v, and $\zeta'_{\rm eff}$ only two can be determined independently.[32] Since for the various bands of a given complex A''_0 has to be constant, while A'_v and $\zeta'_{\rm eff}$ will vary slightly with van der Waals excitation, we constrain A''_0 throughout.

The determination of a reasonable value of A''_0 has to rely on additional arguments.[32] From the lack of asymmetry splitting discussed above, it follows that the rare gas atom sits on average on the symmetry axis (c axis) of the oblate symmetric top benzene. This axis is identical to the a axis of the prolate top complex and therefore A''_0(complex) $\approx C''_0$(benzene). The value of C''_0 for the benzene monomer has not yet been determined experimentally for analogous reasons to the ones discussed for the complex. Benzene is, however, generally believed to be planar and therefore C''_0(benzene) $\approx B''_0$(benzene)/2. So, we set A''_0 of the complex equal to $B''_0/2$ of the benzene monomer.[50,51]

The spectrum of the 6_0^1 band of $C_6H_6\cdot Ar$ is shown in the lower part of Fig. 4. A typical perpendicular band, this spectrum has been previously reported and analyzed.[32] A regular system of red-shaded Q subbranches ($\Delta J=0$; K' and ΔK constant) is found in the middle of the spectrum. The P branch ($\Delta J=-1$) and R branch ($\Delta J=+1$) lines are found in the region around -40 GHz and $+40$ GHz, respectively. This pattern of lines is caused by the $\Delta K=\pm1$ selection rule.

The only significant variation in the overall appearance of a perpendicular band of $C_6H_6\cdot Ar$ can be caused by a change in the value of the Coriolis coupling constant $\zeta'_{\rm eff}$. To demonstrate this point, we show in the upper part of Fig. 4 the spectrum of the 16_0^2 band[34] for comparison. The compression of the P and R branches is quite obvious; additionally the spacing of the Q subbranches is drastically reduced (see the subbranches connected by the dashed lines). This change corresponds to a change from $\zeta'_{\rm eff} = -0.5869$ for the 6_0^1 band to $\zeta'_{\rm eff} = -0.0059$ for the 16_0^2 band. Neglecting the centrifugal terms in Eq. (1), the spacing of neighboring Q branches can be calculated to be

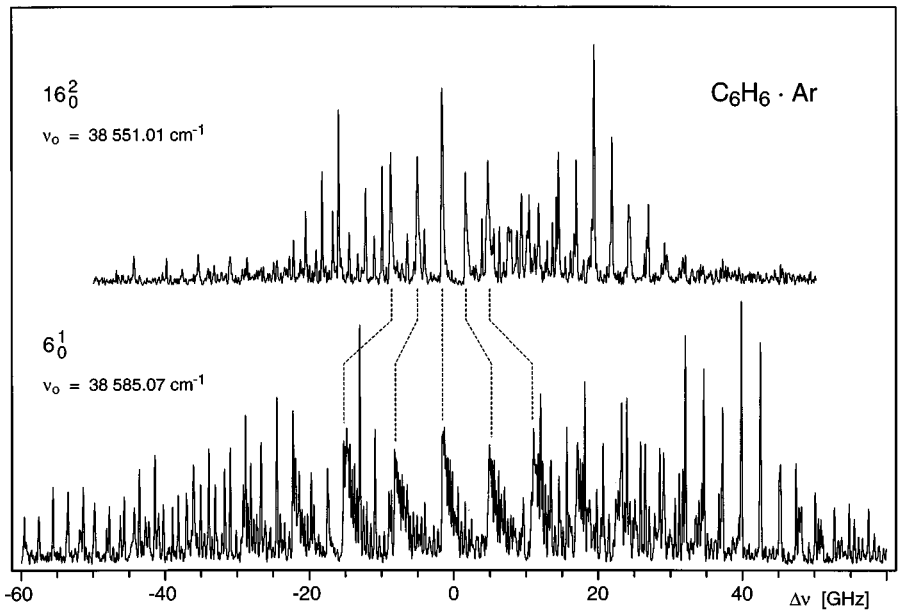

FIG. 4. Rotationally resolved mass-selected resonance-enhanced two-photon ionization spectra of the 6_0^1 and 16_0^2 bands of $C_6H_6 \cdot Ar$. The differing Coriolis coupling constant in the two respective upper vibronic states strongly influences the spacing between the Q-subbands. The corresponding subbands with equal values of K and ΔK are connected by dashed lines.

$$\delta E_Q(K\Delta K+1,K\Delta K)\,\delta E_Q(K\Delta K+1,K\Delta K)$$
$$=2\Delta AK+(A'+A''-B'-B'')-2A'\zeta'_{\text{eff}}. \quad (2)$$

For $C_6H_6 \cdot Ar$ this amounts (in GHz) to

$$\delta E_Q(K\Delta K+1,K\Delta K)$$
$$=-0.241\cdot K\Delta K+3.187-5.452\cdot\zeta'_{\text{eff}}. \quad (3)$$

In other words, the spacing is a sum of a constant term, a small term proportional to $K\cdot\Delta K$, and a dominant term proportional to ζ'_{eff}. Since for a fundamental vibration ζ'_{eff} can already span the range of -1 to $+1$, even a change in the ordering of the subbranches is possible.

The less pronounced shading of the Q subbranches in the 16_0^2 band (as compared to the 6_0^1 band) is caused by an additional small change of the rotational constant B'_v. In general, the shading is given by the relative position $\delta E_Q(J')$ of lines in a Q subbranch

$$\delta E_Q(J')=(B'-B'')J'(J'+1). \quad (4)$$

Owing to this simple relationship, the shading of the Q branches can be used directly to determine the change of the rotational constant B upon vibronic excitation.

C. Rotationally resolved spectra of the van der Waals bands of $C_6H_6 \cdot Ar$

1. The band at $\delta\nu=+40.1$ cm^{-1}

The rotationally resolved spectrum of the strongest van der Waals band of $C_6H_6 \cdot Ar$ at $\delta\nu=+40.1$ cm^{-1} is shown in the upper trace of Fig. 5. The observed linewidth of 130 MHz is solely due to the laser bandwidth and the residual Doppler broadening in the molecular beam. This has been verified by comparison of the observed line shapes with the ones observed for either the 6_0^1 band of the complex or the 6_0^1 band of the monomer. Within the experimental accuracy, no difference is found. In addition, the numerical convolution of the optically measured linewidth of 120 MHz of our laser and the residual Doppler width calculated from the collimation ratio in the jet add up to the observed experimental linewidth. In other words, there is no sign of a contribution by lifetime broadening for this band leading to a combination state of intramolecular vibronic excitation (6^1 state of the benzene substrate) and an intermolecular van der Waals vibration.

The rotational contour of the band is quite similar to that of the 6_0^1 band (see Fig. 4). Clearly, a perpendicular band is observed, leading again to a degenerate upper state. The only two significant differences are that the shading of the Q subbranches is practically absent and that the rotational temperature is lower, presumably due to the increased backing pressure in the jet expansion The spacing of the Q branches is practically unchanged. Thus, the upper vibronic state observed in this band has a Coriolis coupling constant very close to that of the 6^1 state. From the lack of Q branch shading it is concluded that B'_v must be nearly identical to B''_0.

With this information in mind, the assignment of the spectrum is straightforward. A total of 136 unblended rovibronic lines were found and used in the fit of the rotational constants. The results are shown in Table II together with the spectroscopic constants of the previously analyzed bands.[32,34] The constants for these bands were refitted with the recently reported higher precision ground state constants (see Sec. III B and Table I) for consistency.

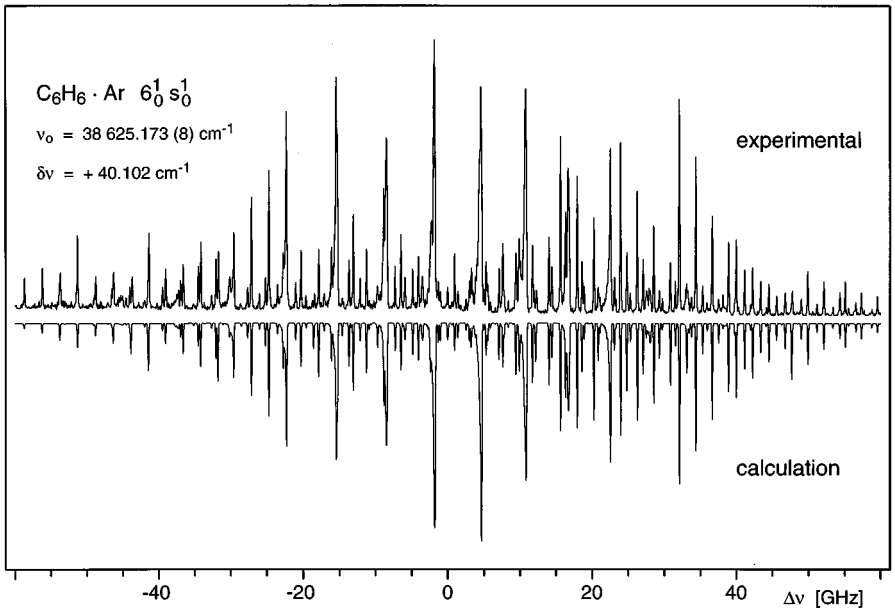

FIG. 5. Comparison between the rotationally resolved experimental recording of the van der Waals band of $C_6H_6 \cdot Ar$ at $\delta\nu = +40.1$ cm^{-1} and the spectrum calculated from the rotational constants fitted to the experimentally observed lines positions. For details see text.

The observed band at $\delta\nu = +40.1$ cm^{-1} shows no signs of isolated perturbations due to possible coupling with background states. This is seen from both the very low value of 23.7 MHz for the standard deviation σ of the fit and the comparison of the experimental spectrum (upper trace of Fig. 5) to the calculated spectrum (lower trace of Fig. 5).

2. The band at $\delta\nu = +62.9$ cm^{-1}

The rotationally resolved spectrum of the van der Waals vibronic band of $C_6H_6 \cdot Ar$ at $\delta\nu = +62.9$ cm^{-1} is shown in Fig. 6. Comparing it to the 6_0^1 band and the van der Waals band at $\delta\nu = +40.1$ cm^{-1}, we find again the same general appearance; a perpendicular band with a similar value of the Coriolis coupling constant. However, the blue shading of the Q subbranches in the 6_0^1 band that vanished in the band at 40.1 cm^{-1} has now become a red shading, indicating a further decrease of B_v'.

The assignment of 107 unblended lines with 130 MHz width was straightforward. The derived values of the inertial constants are reported in Table II. The suspected change in B_v' and the nearly unchanged value of ζ_{eff}' are confirmed. The small value of σ again shows that there are no perturbations in the rotational structure; i.e., that there is no detectable rotationally selective coupling to background states. The regular structure can also be seen by visual comparison between the experimental spectrum and the spectrum calculated with the fitted constants (lower part of Fig. 6). For better comparison, part of the Q branch is shown on an expanded frequency scale in the upper part of Fig. 6.

TABLE II. Spectroscopic constants derived from fits of various vibronic bands of $C_6H_6 \cdot Ar$. ν_0 is the band origin, A_v' and B_v' are the rotational constants, and ζ_{eff}' is the Coriolis coupling constant for the degenerate vibronic state. N refers to the number of assigned lines used in the fit with a mean residual deviation σ of the transitions. $\delta\nu$ is the shift of the combination bands from on the 6_0^1 band. δA and δB are the differences between the observed rotational constants and those of the 6^1 state.

	$C_6H_6 \cdot Ar$					
	16_0^2	6_0^1	$6_0^1 b_0^1$	$6_0^1 s_0^1$	$6_0^1 b_0^2$	$6_0^1 1_0^1$
ν_0 (cm^{-1})	38 551.005	38 585.071	38 616.2	38 625.173	38 647.953	39 509.202
$\delta\nu$ (cm^{-1})	⋯	0.000	31.2	40.102	62.882	924.131
A_v' (cm^{-1})	0.091 195	0.090 862	⋯	0.091 203	0.092 211	0.090 996
B_v' (cm^{-1})	0.039 769	0.040 090	⋯	0.039 149	0.038 332	0.040 049
δA (cm^{-1})	+0.000 333	±0.000 000	⋯	+0.000 341	+0.001 349	+0.000 134
δB (cm^{-1})	−0.000 321	±0.000 000	⋯	−0.000 941	−0.001 758	−0.000 041
ζ_{eff}'	−0.005 9	−0.586 9	⋯	−0.584 9	−0.573 4	−0.555 5
N	53	224	⋯	136	107	118
σ (MHz)	22.1	28.1	⋯	23.7	28.5	30.6

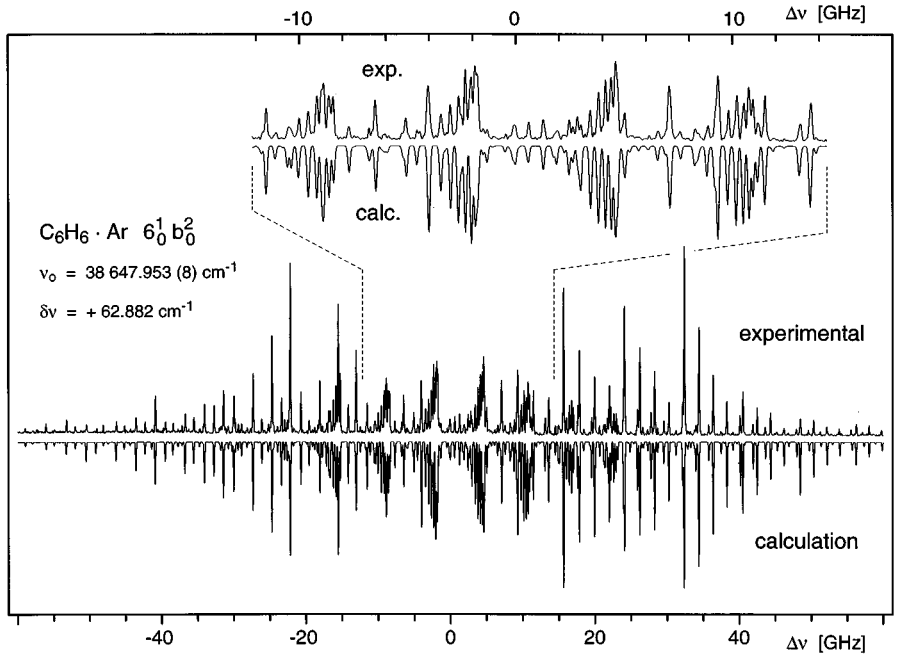

FIG. 6. Comparison between the rotationally resolved experimental recording of the van der Waals band of $C_6H_6 \cdot Ar$ at $\delta\nu = +62.9\ cm^{-1}$ and the spectrum calculated from the rotational constants fitted to the experimentally observed lines positions. For details see text.

3. The band at $\delta\nu = +31.2\ cm^{-1}$

Unlike the two van der Waals bands of $C_6H_6 \cdot Ar$ analyzed so far, the lowest energy band at $\delta\nu = +31.2\ cm^{-1}$ cannot be assigned and understood so easily. Despite its low intensity (only 1.2% of the 6_0^1 band), a highly resolved spectrum (130 MHz linewidth) of good quality was obtained. It is shown in the upper trace of Fig. 7. Its structure differs considerably from the well-understood spectra of the 6_0^1 band

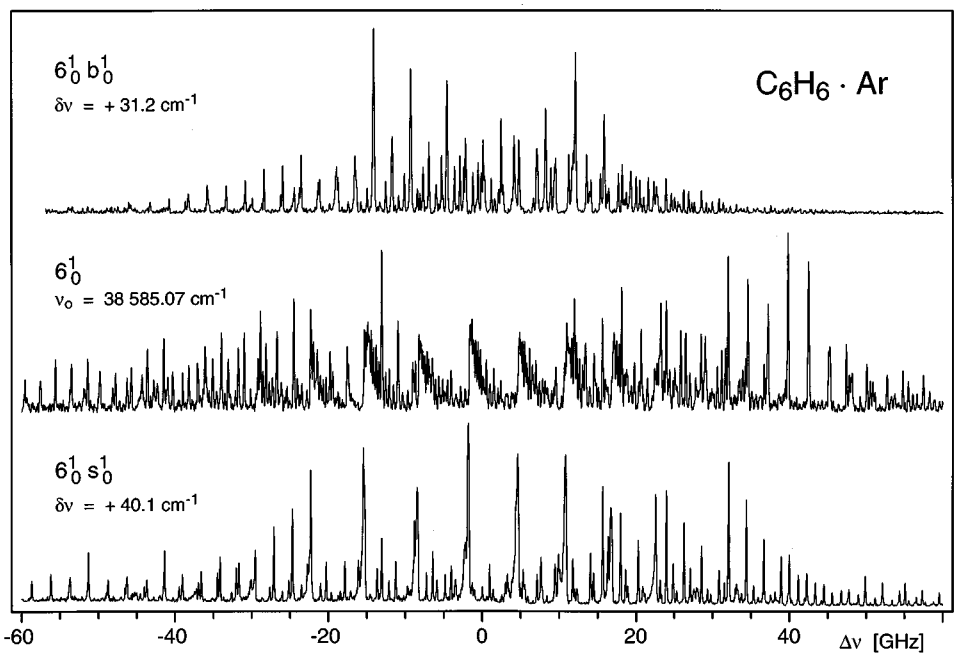

FIG. 7. Comparison of the rotational structure of the vibronic bands of $C_6H_6 \cdot Ar$ at $\delta\nu = +40.1\ cm^{-1}$ (lower trace) and $+31.2\ cm^{-1}$ (upper trace) to the structure of the 6_0^1 band (middle trace). The $6_0^1 s_0^1$ band at $+40.1\ cm^{-1}$ shows a comparable structure of the P branch (around -40 GHz) and the R branch (around $+40$ GHz) and a nearly unchanged spacing of the Q subbranches (around 0 GHz). Only the shading of the Q subbranches is significantly changed due to a small change in the value of B_v'. In contrast, the band at $+31.2\ cm^{-1}$ van der Waals excitation displays a totally different rotational structure as discussed in the text.

(middle trace) and the band at $+40.1$ cm^{-1} (lower trace). This is similar to the situation in *p*-DFB–Ar. Here, the *a*-type rotational structure of the $b_{y_0^1}$ band at $\delta\nu=+33.7$ cm^{-1} was found to differ from that of the *c*-type fundamental band,[39,41] owing to the Herzberg–Teller activity of the short in-plane bending mode in *p*-DFB–Ar.

The experimental conditions used for the recording of the 31.2 cm^{-1} band in $C_6H_6\cdot$Ar were identical to the ones used for the two other van der Waals bands. We can therefore be sure that the new spectrum should have about the same rotational temperature. Qualitatively, a number of differences are observed.

(1) The total width of the spectrum is significantly reduced.
(2) The strikingly regular pattern of *Q* subbranches with nearly identical spacing is replaced by a number of extremely strong spectral features in the middle part of the spectrum with seemingly irregular spacing and increasing intensity to the sides.
(3) There is a pile up of strong lines near the middle of the spectrum.

All of these features make the interpretation of the band as a perpendicular band impossible. From the previously determined rotational constants of the other bands of $C_6H_6\cdot$Ar, we have a very good understanding of how strongly these constants might be affected by intramolecular or van der Waals excitation. The influence of the Coriolis coupling constant also is well understood (Sec. III B). Despite numerous attempts, even the major features could not be reproduced by perpendicular selection rules. Rotationally selective coupling to a second van der Waals state and the consequent perturbation of the rotational structure can be excluded due to the low energy of the observed state. The influence of coupling to a different intramolecular state should not perturb the rotational structure to an extreme degree (see Sec. IV B).

The only other alternative would be a parallel transition with different selection rules ($\Delta K=0$). Such a transition must lead to a nondegenerate vibronic state that does not possess any Coriolis splitting into substates. The only free parameters for such a band are the rotational constants A_v' and B_v'. Appropriate calculations were performed and no kind of similarity to the experimental spectrum was found with reasonable values of A_v' and B_v'. This means that the observed band also cannot be interpreted as a straightforward parallel transition.

With neither a perpendicular nor a parallel band structure found, a more complicated model is needed for the interpretation of the band at $\delta\nu=+31.2$ cm^{-1}. The search for the appropriate vibronic state structure and coupling mechanism will be described in the accompanying paper.[42]

D. Rotationally resolved spectra of the van der Waals bands of $C_6H_6\cdot{}^{84}Kr$

Additional information on the benzene–rare gas complexes can be derived from spectra with either the rare gas atom changed[33] or by isotopic substitution of the benzene part. We have performed both experiments. The isotopic substitution of benzene changes the high frequency intramolecular modes and only slightly the intermolecular modes. The rare gas atom, on the other hand, influences mainly the low frequency intermolecular ones. As a consequence, a much smaller change in the total level structure of the complex will be caused by the exchange of the rare gas atom. We therefore first discuss the spectra of $C_6H_6\cdot{}^{84}Kr$ before turning to the spectra of $C_6D_6\cdot$Ar.

1. The band at $\delta\nu=+37.4$ cm^{-1}

The rotationally resolved spectrum of $C_6H_6\cdot{}^{84}Kr$ at $\delta\nu=+37.4$ cm^{-1} is shown in the middle trace of Fig. 8. Its experimental quality is not as high as found for the bands of $C_6H_6\cdot$Ar in agreement with our previous experience with this cluster.[33] There is, however, no sign of broadening in the spectrum. We can conclude from this that $C_6H_6\cdot{}^{84}Kr$ does not show any appreciable dissociation due to the excited van der Waals vibration.

For comparison the previously analyzed spectrum of the 6_0^1 band is also included in Fig. 8. The two spectra are very similar; the only major difference is the reduced shading of the *Q* branches. This is in line with the observations for $C_6H_6\cdot$Ar reported above. Because of the strong overlap of lines in the *Q* branches only 95 unblended lines could be assigned and used in the determination of the spectroscopic constants. These are reported in Table III. The standard deviation of the fit is quite small and we conclude that there are no perturbations present in the spectrum. This was also confirmed by visual comparison of the experimental spectrum with a spectrum calculated from the newly determined spectroscopic constants. All significant lines predicted can be found in the observed spectrum and all observed transitions are indeed predicted. In addition, we infer that there is no selective fast dissociation of single rotational states that would lead to a disappearance of the appropriate lines.

2. The band at $\delta\nu=+65.1$ cm^{-1}

The van der Waals band of $C_6H_6\cdot{}^{84}Kr$ at $\delta\nu=+65.1$ cm^{-1} is about a factor of 6 weaker than the one at 37.4 cm^{-1}. However, a reasonable quality sub-Doppler spectrum could still be measured. It is shown in the upper trace of Fig. 8. Comparison with the other two spectra shows a very similar rotational structure, with only the slight blue shading of the *Q* branches changed to a slight red shading with increased van der Waals excitation.

Owing to the similarity of this spectrum to the previously analyzed ones, we expected the assignment to be straightforward. Indeed, a large fraction of the observed lines could be assigned within a consistent model. However, many of the observed lines are not found at consistent positions and/or show strengths that deviate considerably from expectation. Three possible causes have to be discussed.

(1) The quality of the experimental spectrum could in principle be too low for the unambiguous determination of lines. We therefore checked the calibration of the spec-

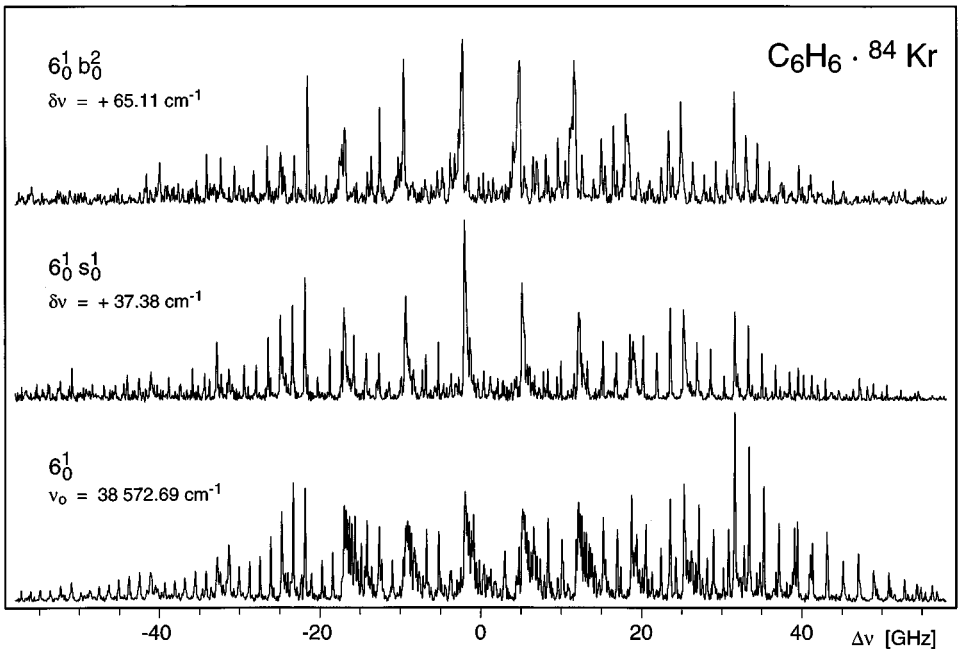

FIG. 8. Comparison of the rotational structure of the vibronic bands of $C_6H_6 \cdot {}^{84}Kr$ at $\delta\nu = +37.38$ cm^{-1} (middle trace) and $+65.11$ cm^{-1} (upper trace) to the structure of the 6_0^1 band (lower trace). Both bands with additional excitation of van der Waals modes show a comparable structure of the *P* branch (around -30 GHz) and the *R* branch (around $+30$ GHz) and a nearly unchanged spacing of the *Q* subbranches (around 0 GHz). Only the shading of the *Q* subbranches is significantly changed due to small changes in the value of B_v'.

trum very carefully and looked at previously analyzed spectra of very weak transitions. It was clearly found that the deviations encountered are significant.

(2) Our assignment may be systematically off by one unit in either the J or K values. To confirm the assignment, all the regular patterns in the *P* and *R* branch were identified and analyzed in a fashion described previously for the highly perturbed $6_0^1 1_0^3$ band of C_6H_6.[52] At the low rotational temperature known from the analysis of the other spectra, not many choices for the quantum numbers are possible and each value of J' for a particular line allows the prediction of the consequent position of the associated line in the *Q* branch using only the precisely known value of B_0''. Since the sharp *Q* branches are readily identified, all but one assignment could be excluded in most cases and an unambiguous determination of the value of J' was possible for a large number of lines. Since each system of lines in the *R* branch with constant K' has to start with the $J' = K'$ line, the K' assignment also follows directly. 74 unblended lines could be securely assigned in this fashion.

(3) The only remaining possibility that comes to mind is that we observe fairly severe perturbations in the spectrum. Additional proof for this supposition comes from the quality of the fit of the spectroscopic constants to the observed line positions. When all 74 lines are used, a standard deviation of 55.4 MHz results, more than a factor of 2 worse than is usually found for our sub-Doppler spectra. Elimination of eight of the lines used in the fit reduces this value to 34.1 MHz. However, a careful examination shows that the assignment of these particular lines is secure. For comparison, both sets of constants determined are included in Table III and it can be seen that they do not differ by large amounts. An analysis of the residuals of the individual lines shows particularly strong and systematic deviations from the expected position for lines leading to $|K' = 2, -l\rangle$ and $|K' = 3, -l\rangle$ states.

TABLE III. Spectroscopic constants derived from fits of various vibronic bands of $C_6H_6 \cdot {}^{84}Kr$. For an explanation of the various symbols see Table II. For the $6_0^1 b_0^2$ band two sets of constants are shown corresponding to differing sets of lines. For details see text.

	$C_6H_6 \cdot {}^{84}Kr$			
	6_0^1	$6_0^1 s_0^1$	$6_0^1 b_0^2$	
ν_0 (cm^{-1})	38 572.692	38 610.072	38 637.798	
$\delta\nu$ (cm^{-1})	0.000	37.380	65.106	
A_v' (cm^{-1})	0.090 836	0.091 054	0.092 232	0.092 249
B_v' (cm^{-1})	0.027 245	0.026 811	0.026 178	0.026 171
δA (cm^{-1})	±0.000 000	+0.000 218	+0.001 396	+0.001 413
δB (cm^{-1})	±0.000 000	−0.000 434	−0.001 067	−0.001 074
ζ_{eff}'	−0.586 4	−0.584 3	−0.550 4	−0.549 9
N	150	95	74	66
σ (MHz)	22.6	21.7	55.4	34.1

In summary, we believe that the van der Waals band of $C_6H_6 \cdot {}^{84}Kr$ at $\delta\nu = +65.1$ cm^{-1} is significantly perturbed. Owing to the large $S_1 - T_1$ separation of 8464 cm^{-1} in benzene, intersystem crossing is known to proceed in the statistical limit[53] and singlet–triplet coupling cannot be a source

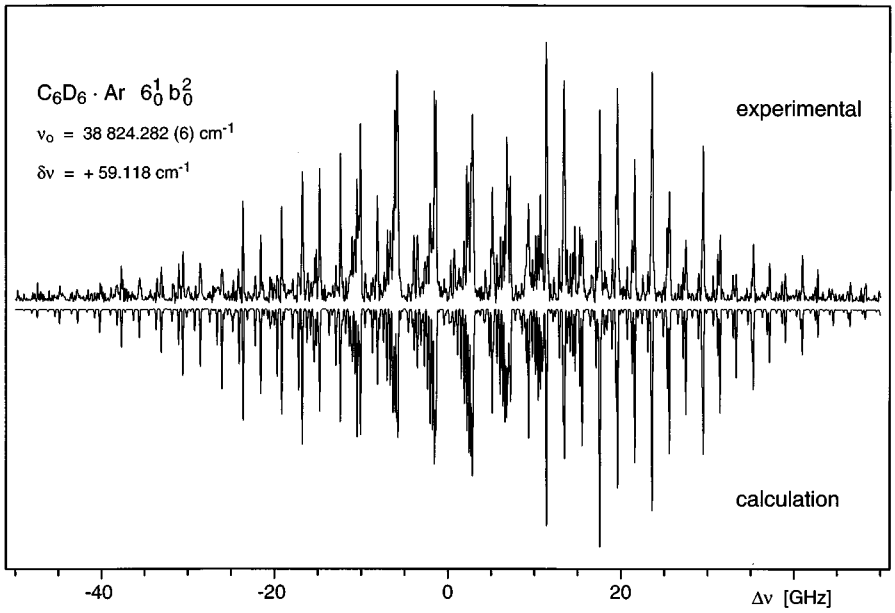

FIG. 9. Comparison between the rotationally resolved experimental recording of the van der Waals band of $C_6D_6 \cdot Ar$ at $\delta\nu = +59.1$ cm^{-1} and the spectrum calculated from the rotational constants fitted to the experimentally observed lines positions. For details see text.

of the very selective coupling. Possible alternative perturbers will be discussed below together with the implications of this supposition.

E. Rotationally resolved spectra of the van der Waals bands of $C_6D_6 \cdot Ar$

1. The band at $\delta\nu = +59.1$ cm^{-1}

The rotationally resolved spectrum of the van der Waals band of $C_6D_6 \cdot Ar$ is shown in Fig. 9. The new spectrum clearly shows the rotational structure of a perpendicular transition. The spacing of the Q branches is nearly identical to that found for the 6_0^1 band. The turn around of shading is quite similar to the situation found in $C_6H_6 \cdot Ar$. A detailed analysis shows that the apparent reduction of the number of lines is actually due to a frequent overlap of lines.

A total of 92 unblended lines could be assigned since the Q branch shading is sufficiently large to allow assignment of individual lines. The constants determined from the observed line positions are summarized in Table IV. The standard deviation of the fit shows no indication of perturbations in the spectrum. The calculated spectrum shown in the lower part of Fig. 9 matches the experimental one nicely.

2. The band at $\delta\nu = +39.7$ cm^{-1}

The experience gained from the van der Waals bands of $C_6H_6 \cdot Ar$ and $C_6H_6 \cdot {}^{84}Kr$ allows the prediction that the spectrum of the band of $C_6D_6 \cdot Ar$ at $+39.7$ cm^{-1} should be unperturbed and display a small shading of the Q branches. However, a casual inspection of the experimental spectrum in Fig. 10 shows that this band has a Q branch shading quite similar to the band at 59.1 cm^{-1} and accordingly a similar value of B_v'.

The assignment of individual lines in this spectrum proved to be far from trivial. All the checks and precautions explained above for the band of $C_6H_6 \cdot {}^{84}Kr$ at 65.1 cm^{-1} were performed. As a result 82 lines, believed to be unblended, were assigned and used in the fit of the spectroscopic constants. These are listed in Table IV. The standard deviation of the fit is 96.6 MHz, about a factor of 4 worse than found for most other spectra. This means that the average deviation between the expected and the observed positions of even the assigned lines is nearly a full linewidth. Some hints of a systematic behavior can be found in a detailed analysis of the residuals.

To demonstrate the observed irregularity in the experimental spectrum more clearly, it is displayed in Fig. 10 on an expanded frequency scale. Both the part for $\Delta\nu \leqslant 0$ GHz (shown in the upper half of the figure; upper scale) and the part for $\Delta\nu \geqslant 0$ GHz (shown in the lower half of the figure; lower scale) is compared to the calculation using the con-

TABLE IV. Spectroscopic constants derived from fits of various vibronic bands of $C_6D_6 \cdot Ar$. For an explanation of the various symbols see Table II.

	$C_6D_6 \cdot Ar$			
	6_0^1	$6_0^1 b_0^1$	$6_0^1 s_0^1$	$6_0^1 b_0^2$
ν_0 (cm^{-1})	38 765.164	38 794.3	38 804.837	38 824.282
$\delta\nu$ (cm^{-1})	0.000	29.1	39.673	59.118
A_v' (cm^{-1})	0.075 440	⋯	0.076 096	0.076 420
B_v' (cm^{-1})	0.037 710	⋯	0.036 333	0.036 271
δA (cm^{-1})	±0.000 000	⋯	+0.000 656	+0.000 980
δB (cm^{-1})	±0.000 000	⋯	−0.001 377	−0.001 439
ζ_{eff}'	−0.395 5		−0.408 8	−0.389 4
N	117	⋯	82	92
σ (MHz)	20.7	⋯	96.6	27.6

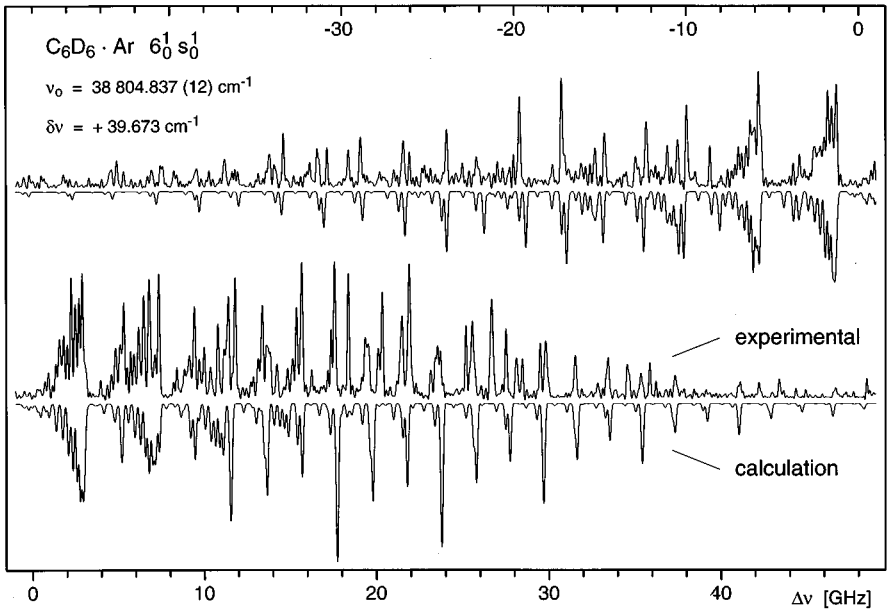

FIG. 10. Comparison between the rotationally resolved experimental recording of the van der Waals band of $C_6D_6 \cdot Ar$ at $\delta\nu = +39.7\ cm^{-1}$ and the spectrum calculated from the rotational constants fitted to the experimentally observed lines positions. Note the agreement for the major portion of the spectrum and also the significant disagreement for a considerable fraction of the observed lines. For a discussion, see the text.

stants fitted to the observed line positions. A large number of the individual features agree and so does the overall structure of the spectrum. However, a fair number of lines are also missing and/or shifted in the experimental spectrum. We were, for example, unable to locate any of the lines leading to $|K'=2,-l\rangle$ and $|K'=4,+l\rangle$ states, even though they should be quite strong at the rotational temperature observed. This provides clear evidence that the strongest van der Waals band of $C_6D_6 \cdot Ar$ leading to a state of moderate intramolecular excitation is highly perturbed. The implications of this observation will be discussed below.

3. The band at $\delta\nu = +29.1\ cm^{-1}$

The lowest excitation energy van der Waals band of $C_6D_6 \cdot Ar$ is similar to that found for $C_6H_6 \cdot Ar$. The experimental spectrum around $\delta\nu = +29.1\ cm^{-1}$ is displayed in the upper trace of Fig. 11. Also shown in Fig. 11 for comparison are the two bands of $C_6D_6 \cdot Ar$ which were found to have a regular and unperturbed perpendicular band structure (6_0^1 band in the middle and the $+59.1\ cm^{-1}$ band on the bottom). All the observations made for the general appearance of the corresponding band of $C_6H_6 \cdot Ar$ (see Sec. III C 3) apply here as well. Our attempts to assign this spectrum with a perpendicular or parallel band model were equally unsuccessful. Indeed, the lowest energy van der Waals spectra of both clusters are very similar, except for a contracted scale for the deuterated cluster that is not unexpected as the heavier isotope possesses smaller rotational constants. It will be shown in the accompanying paper[42] that this similarity is not accidental but rather that the spectral complexity in both cases has the same spectroscopic cause.

IV. DISCUSSION

In the preceding sections the rotationally resolved spectra of the various van der Waals bands were spectroscopically analyzed without specific reference to the particular identity of the upper vibronic state of each band. This was done purposely as we want to draw unprejudiced conclusions from the observed experimental facts. Only the identity of the cluster, as deduced from the mass selection in the experiment, and its ground state rotational constants, as determined by microwave spectroscopy, were used so far. The various low frequency van der Waals vibrations excited in combination with the 6^1 state do not influence the frequency of ν_6 and the other high frequency intramolecular vibrational modes to a significant degree. We therefore take the shift $\delta\nu$ of each van der Waals band from the 6_0^1 band of the benzene–rare gas complex to be equal to the energy of the corresponding van der Waals level.

A. The vibronic identity of the van der Waals states

The particular band type observed for each rotationally resolved vibronic transition severely limits the possible symmetries of the accessed van der Waals level. This is a consequence of the high symmetry (C_{6v}) of benzene–rare gas clusters and the low van der Waals energies considered. The lack of asymmetry splitting of individual rovibronic transitions (cf. Sec. III B) proves that the complexes are symmetric tops in both electronic states. This is confirmed by the absence of the electronic origin transition.[2,46,47] Garrett *et al.* have discussed this issue in recent work and concluded that benzene–Ar is indeed correctly described by a C_{6v} structure.[47] The only change that occurs upon electronic excitation is a slight change in the van der Waals bond length.[32]

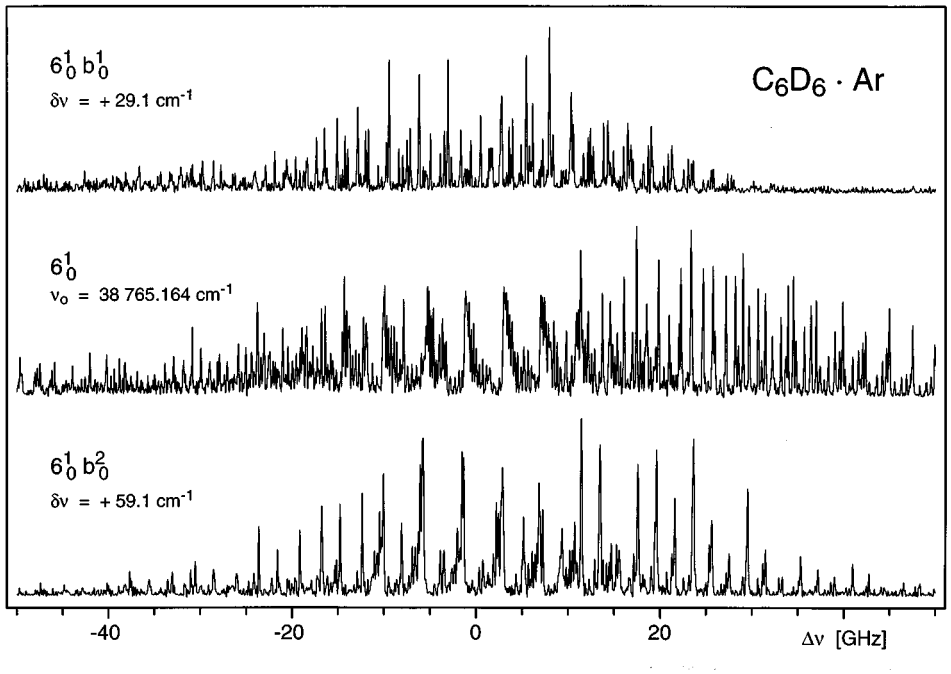

FIG. 11. Comparison of the rotational structure of the vibronic bands of $C_6D_6 \cdot Ar$ at $\delta\nu = +59.1$ cm^{-1} (lower trace) and $+29.1$ cm^{-1} (upper trace) to the structure of the 6^1_0 band (middle trace). The band at $+59.1$ cm^{-1} shows a comparable structure of the *P* branch (around -25 GHz) and the *R* branch (around $+25$ GHz) and a nearly unchanged spacing of the *Q* subbranches (around 0 GHz). Only the shading of the *Q* subbranches is significantly changed due to a small change in the value of B'_v. In contrast, the band at $+29.1$ cm^{-1} van der Waals excitation displays a totally different rotational structure as discussed in the text.

As a consequence, only a few transitions to some of the lowest van der Waals levels can be observed.

Benzene–rare gas clusters have two van der Waals vibrational modes, the totally symmetric (a_1) stretching vibration *s* along the symmetry axis of benzene and the degenerate (e_1 symmetry) bending vibration or librational motion *b*. This leads to a series of overtone and combination levels with easily derived symmetry, the first few of which are listed in Table V. Besides the nomenclature $b^n s^m$ used for spectra of polyatomic molecules, we also show the notation of van der Avoird,[26] where *n* is the number of bend quanta, *l* is the vibrational angular momentum, and n_z is the number of stretch quanta. $\Gamma(|S_0,n,l,n_z\rangle)$ is the symmetry of the pure van der Waals level and is identical to the symmetry in the S_0 state with no intramolecular vibrational excitation. Since the purely electronic $S_1 \leftarrow S_0$ transition is symmetry forbidden in benzene and its rare gas clusters, a false origin built onto the 6^1 state is observed and the 6^1_0 band is the strongest transition in the one-photon spectrum of the clusters. As a consequence, we have to consider the symmetry of combination states built from the benzene 6^1 state and the various van der Waals levels to determine the allowed transitions. $\Gamma(|S_1+\nu_6,n,l,n_z\rangle)$ is shown in the last column of Table V.

TABLE V. Symmetry of the lowest van der Waals states of benzene–rare gas clusters. Shown are both the spectroscopic notation for the states [e.g., $b^1(l=1)s^1$ for the state with 1 quantum of bend excitation, vibrational angular momentum $l=1$ and 1 quantum of stretch excited] and the notation of van der Avoird (Ref. 26), where *n* is the number of bend quanta, *l* is the vibrational angular momentum, and n_z is the number of stretch quanta. $\Gamma(|S_0,n,l,n_z\rangle)$ is the symmetry of the pure van der Waals state and is identical to the symmetry in the S_0 state with no intramolecular excitation. $\Gamma(|S_1+\nu_6,n,l,n_z\rangle)$ is the symmetry of the combination of van der Waals state and electronically excited 6^1 state.

C_{6v}	n	l	n_z	$\Gamma(\|S_0,n,l,n_z\rangle)$	$\Gamma(\|S_1+\nu_6,n,l,n_z\rangle)$
g.s.	0	0	0	A_1	E_1
$b^1(l=1)$	1	±1	0	E_1	$A_1+A_2+E_2$
s^1	0	0	1	A_1	E_1
$b^2(l=2)$	2	±2	0	E_2	$B_1+B_2+E_1$
$b^2(l=0)$	2	0	0	A_1	E_1
$b^1(l=1)s^1$	1	±1	1	E_1	$A_1+A_2+E_2$
s^2	0	0	2	A_1	E_1
$b^3(l=3)$	3	±3	0	B_1+B_2	$2E_2$
$b^3(l=1)$	3	±1	0	E_1	$A_1+A_2+E_2$

With $\Gamma(T_z)=A_1$ and $\Gamma(T_{x,y})=E_1$ in the point group C_{6v}, perpendicular transitions are allowed to vibronic states with total symmetry E_1 and parallel transitions are allowed to states with total symmetry A_1. Perpendicular transitions have been found exclusively in benzene.[45] The strongest ones are due to the Herzberg–Teller inducing modes of e_{2g} symmetry (total symmetry E_{1u} together with the B_{2u} symmetry of the S_1 state), primarily ν_6. Parallel transitions have not yet been identified in the spectrum of benzene. Inspection of Table V shows that for $C_6H_6 \cdot Ar$ we can expect perpendicular transitions in the vicinity of the perpendicular 6^1_0 band that lead to either the $6^1(l=\mp 1)s^1$ or $6^1(l=\mp 1)s^2$ states and to the $6^1(l=\pm 1)b^2(l=\pm 2)$ states or the $6^1(l=\pm 1)b^2(l=0)$ states. A parallel band could in principle

TABLE VI. Assignment of the van der Waals states built onto the 6^1 state of $C_6H_6 \cdot Ar$ according to various authors. For explanation see text.

Energy of vdW state (cm^{-1})	Menapace and Bernstein[a]	Bludský *et al.*[b]	Weber[c]	van der Avoird[d]
31.2	b^2	b^1	(b^2)	b^1
40.1	s^1	s^1	s^1	s^1
62.9	b^4	b^2 or b^1s^1	s^2	b^2

[a]Reference 2.
[b]Reference 25.
[c]Reference 54.
[d]Reference 26.

be observed to the substate of $6^1(l=\pm 1)b^1(l=\pm 1)$ with total symmetry A_1.

A number of authors made assignments of the three van der Waals bands of $C_6H_6 \cdot Ar$ observed in the low resolution spectrum. Their results are summarized in Table VI. All authors agree on the assignment of the band at 40.1 cm^{-1} as the $6_0^1 s_0^1$ transition. The main arguments used were the good match with the predicted frequencies of the s^1 level and the strong intensity observed in the experimental spectrum. This intensity is thought to be due to a favorable Franck–Condon factor, in line with the slight shortening of the benzene–Ar bond upon electronic excitation.[32] The rotational analysis presented in Sec. III C 1 indeed shows a perpendicular band, as expected. For the Coriolis coupling constant ζ_{eff} no significant change is predicted between the 6^1 state and the 6^1s^1 state as the stretch mode is nondegenerate and therefore cannot contribute to ζ_{eff}. This is nicely confirmed by the experimental observation (cf. Table II) and we can accept this assignment.

Less agreement is found for the assignment of the band at 31.2 cm^{-1}. Experimental investigations[2,54] favor its assignment as the $6_0^1 b_0^2$ transition for several reasons. First, original calculations place the bend frequency at about 11 cm^{-1} (Ref. 2) and the first overtone at 22 cm^{-1}, reasonably close to the observed value of 31 cm^{-1}. Second, the overtone combination 6^1b^2 contains an component of vibronic symmetry E_1 for both the $l=0$ and $l=2$ substates and would therefore be expected to derive intensity from both Franck–Condon activity and Fermi resonance with the 6^1s^1 state. In addition, an analogous assignment was made for the corresponding band in the closely related system *p*-DFB–Ar.[3,4] More recent 3D calculations for $C_6H_6 \cdot Ar$,[25,26,55] on the other hand, place the frequency of the bend at a much higher value (21 cm^{-1}–33 cm^{-1}). This suggests a $6_0^1 b_0^1$ assignment. The analysis presented in Sec. III C 3 shows that this band is not a simple perpendicular band. This rules out the bend overtone assignment. A recent study of *p*-DFB–Ar (Ref. 41) places the first quantum of the b_y vibration at 33.7 cm^{-1}. However, the band in $C_6H_6 \cdot Ar$ is also not found to be a simple parallel band, so it cannot be solely a bending fundamental. This point will be clarified and discussed in detail in the accompanying paper.[42]

The largest variety of assignments was proposed for the remaining band at 62.9 cm^{-1}. This band is a perpendicular transition with a value of ζ_{eff} that is nearly the same as that of the 6^1 state. We conclude that the upper vibronic state of the transition has to be of total symmetry E_1 and that the van der Waals level included in the combination state is not contributing significantly to ζ_{eff}. The symmetry rules out right away the $6_0^1 s_0^1 b_0^1$ assignment proposed by Bludský *et al.*[25] The assignment of Menapace and Bernstein as $6_0^1 b_0^4$ (Ref. 2) is closely coupled to their assignment of the 31.2 cm^{-1} band as the bend overtone and also is unlikely, owing to the complex coupling schemes expected for such a highly degenerate overtone state. Of the remaining possibilities, both the $6^1(l=\mp 1)s^2$ states and the $6^1(l=\pm 1)b^2(l=0)$ states have the correct symmetry and also Coriolis coupling constant, as neither the nondegenerate stretch nor the $l=0$ substates of the bend overtone will contribute to ζ_{eff}. A decision between the two possibilities cannot be deduced from the rotational analysis alone. It will, however, follow immediately from the assignment of the 31.2 cm^{-1} band. The last remaining possibility, i.e., the $6^1(l=\pm 1)b^2(l=\pm 2)$ states, would have the E_1 symmetry needed to support the perpendicular transition. However, the value of ζ_{eff} is expected to be $\zeta_{\text{eff}} = \zeta_6' + 2 \cdot \zeta_b = 0.59 + 2 \cdot 0.22 = 1.03$, very different from the observed one (cf. Table II). The value of ζ_b used in this estimate was deduced from the calculation of van der Avoird.[26]

In summary, we conclude from the rotational analysis of the three van der Waals bands in $C_6H_6 \cdot Ar$ that the one at 40.1 cm^{-1} is definitively the $6_0^1 s_0^1$ transition. The one at 31.2 cm^{-1} is most likely the $6_0^1 b_0^1$ transition and, as a consequence, the band at 62.9 cm^{-1} is most likely the $6_0^1 b_0^2$ transition. Conversely, assignment of the lower band as $6_0^1 b_0^2$ would lead to the assignment of the higher band as $6_0^1 s_0^2$. The first combination forces one to deviate from the hitherto accepted opinion that all vibronic van der Waals bands draw their intensity from Franck–Condon activity. Instead second-order Herzberg–Teller coupling due to a combination of *intramolecular* and *intermolecular* vibrations would need to be invoked for the appearance of the $6_0^1 b_0^1$ transition. Alternatively, Maxton *et al.* have recently proposed a model where the vibronic intensity derives from the librational motion within the complex.[56] This will be discussed in the accompanying paper.[42] In the second combination the strength of the $6_0^1 s_0^2$ transition would have to be carefully discussed, as it seems far too intense for simple Franck–Condon activity.

The decreases in rotational constants observed for the van der Waals excitation are quite reasonable and similar to the ones predicted by recent calculations.[26] If we interpret changes in B_v' within the framework of a rigid structure, changes of the average distance $\langle r_{\text{Ar}} \rangle$ between the Ar atom and the benzene ring can be determined.[32] They amount to a lengthening of the bond by 53 mÅ for excitation to the state at 40.1 cm^{-1} and one of 101 mÅ for excitation to the state at 62.9 cm^{-1}. In view of the large amplitude motion of the Ar atom relative to the benzene, such an increase seems quite reasonable. The simple picture cannot, however, explain the observed increase in A_v'. This can only be understood in the framework of a complete 3D calculation including the molecular rotation. The rotational constants are then a very important indication as to whether the spatial distribution of the

vibrational wave functions has been determined correctly. This will be discussed in detail in the accompanying paper.[42]

The rotational band structures and the energetic positions of the van der Waals states found for $C_6H_6 \cdot {}^{84}Kr$ and $C_6D_6 \cdot Ar$ are very similar to the ones found for $C_6H_6 \cdot Ar$. All the considerations outlined above for $C_6H_6 \cdot Ar$ should therefore also apply to these two clusters and we propose the same assignments of the van der Waals bands. The increase in van der Waals frequencies for $C_6H_6 \cdot {}^{84}Kr$ corresponds to the stronger binding of this cluster;[20,22] the slight decrease in $C_6D_6 \cdot Ar$ is the usual deuterium effect.

B. Implications for vibrational predissociation

The individual rovibronic lines in all eight reported van der Waals bands showed no broadening beyond that due to the finite laser linewidth and the residual Doppler width in the jet. We can therefore conclude that the various clusters do not predissociate on the time scale of our experiment even with added intermolecular excitation. The excess vibrational energy already present when the 6^1 state is excited by itself is 521 cm^{-1} for $C_6H_6 \cdot Ar$ and $C_6H_6 \cdot {}^{84}Kr$ and 499 cm^{-1} for $C_6D_6 \cdot Ar$.

Calculations place the binding energy D_e'' of S_0 benzene–Ar at 287 cm^{-1},[2] 429 cm^{-1},[20] 393 or 425 cm^{-1},[25] and 408 cm^{-1}.[55] To obtain a value of D_0' relevant for the present discussion, the zero point energy of the van der Waals vibrations of about 50 cm^{-1} (Ref. 26) has to be subtracted from D_e'' to obtain a value for D_0''. In addition, the experimentally observed red shift of 21 cm^{-1} between the 6_0^1 band of the complex and the 6_0^1 band of the bare benzene[2] means that the complex is more tightly bound in the S_1 state by this amount. In other words, $D_0' = D_0'' + 21\ cm^{-1}$. This finally puts D_0' of benzene–Ar into the range 258–400 cm^{-1} and well below the energy of the ν_6' vibration in both $C_6H_6 \cdot Ar$ and $C_6D_6 \cdot Ar$.

Recent mass-selected pulsed field threshold ionization experiments have made possible the experimental determination of upper limits for the dissociation threshold of the ionic complexes.[57] Limits of $D_0' < 361\ cm^{-1}$ for $C_6H_6 \cdot Ar$ and $D_0' < 435\ cm^{-1}$ for $C_6H_6 \cdot {}^{84}Kr$ can be deduced from these. Even for the more tightly bound $C_6H_6 \cdot {}^{84}Kr$, the energy of ν_6' is probably still higher than D_0'.[20,55,57] As a consequence of these various estimates, predissociation should be energetically possible. However, the predissociation rate seems to be too low to cause an observable broadening of individual rovibronic lines. Our spectral resolution puts a lower limit of about 5 ns on the predissociation lifetime.

The predissociation of molecular complexes containing vibrational excitation in excess of the binding energy can either be described by statistical models or by the ''energy/momentum gap'' law. For a statistical model to be applicable, fast intramolecular vibrational relaxation (IVR) has to occur before the unimolecular reaction. As will be discussed below, IVR is at most very restricted for the vibronic levels of benzene–rare gas complexes discussed in this work. Consequently, we will have to turn to an ''energy/momentum gap'' model for a discussion of the observed stability of the complexes.

TABLE VII. Symmetry and vibrational excess energy for the lowest vibrational levels in S_1 benzene. δE denotes the energy difference between the designated level and the 6^1 level.

		C_6H_6		C_6D_6	
State	Symmetry	Excess energy (cm^{-1})	δE (cm^{-1})	Excess energy (cm^{-1})	δE (cm^{-1})
ν_{16}	E_2	238	−283	208	−291
ν_4	B_1	365	−156	306	−193
$2\cdot\nu_{16}$	A_1+E_2	475	−46	416	−83
ν_{11}	A_1	516	−5	382	−117
ν_6	E_2	521	0	499	0
ν_{10}	E_1	581	60	454	−45
$\nu_4+\nu_{16}$	E_1	602	81	514	15
ν_{17}	E_2			590	91
$\nu_{11}+\nu_{16}$	E_2			590	91

Ewing[58] has proposed and discussed a simple universal formula that summarizes the relevant considerations. It predicts the predissociation rate τ^{-1} of molecular clusters to be

$$\tau^{-1} \approx 10^{13} \exp[-\pi(\Delta n_t + \Delta n_r + \Delta n_v)], \tag{5}$$

where Δn_t is the change in the translational quantum number, Δn_r is the change in the rotational quantum number, and Δn_v is the change in the vibrational quantum numbers. All changes are evaluated between the originally excited cluster level and the levels of the fragments. This formula failed initially for the example of *p*-DFB–Ar.[59] However, proper consideration of Fermi resonances gave good agreement between the observed and calculated rates,[59] just as in the related case of *s*-tetrazine–Ar.[58]

To apply this formula to the situation found in benzene–rare gas clusters, we have to examine the possible predissociation channels. They are given by the low lying vibrational levels of S_1 benzene. All the levels expected in the range from zero excess energy to $+100\ cm^{-1}$ above the 6^1 state are shown in Table VII, together with their symmetry and the relevant energy differences δE. A particular channel is open when the vibrational state energy is less than that of 6^1 by at least D_0'. For a likely value of D_0' of about 360 cm^{-1}, Table VII shows that all vibrationally excited channels are closed. Thus, 6^1 benzene–Ar clusters can only dissociate to the vibrationless S_1 benzene, yielding the pair S_1 benzene+Ar with a translational energy E_t of $\leqslant 161\ cm^{-1}$. According to Ewing,[58] the associated translational wave function can be characterized by the quantity

$$q_t = (2\mu_t E_t)^{1/2}/a\hbar, \tag{6}$$

where μ_t is the reduced mass of the cluster and a is the range parameter of a model Morse potential which describes the van der Waals stretching motion that is thought to be the dissociation coordinate. From q_t, the quantity Δn_t needed for the evaluation of Eq. (5) can be calculated using[58]

$$\Delta n_t \approx |q_t/2 - v_t|, \tag{7}$$

where ν_t is the number of excited quanta in the van der Waals stretching mode. Inserting $E_t=161\ \mathrm{cm}^{-1}$ and $a=1.48\ \text{Å}^{-1}$ (Ref. 25) leads to $q_t\approx 11$ and $\Delta n_v=1$ for the dissociation of $6^1\ C_6H_6\cdot Ar$ into the vibrationless benzene fragment. The fastest possible predissociation rate involves no change in rotation; consequently $\Delta n_r=0$. We then calculate a predissociation time τ of 70 μs. Even if this simple estimate is off by one or two orders of magnitude, we see that no line broadening due to predissociation is expected in the rotationally resolved spectrum and why the dispersed fluorescence spectrum of the state reported previously shows no signature of the benzene fragment.[60]

The addition of van der Waals vibrational energy to the cluster does not increase the total vibrational energy content to more than 584 cm^{-1} for the various bands presented in this work. Most likely, still less energy is left to be distributed between the possible fragments than the energy of the lowest energy mode in benzene, ν_{16}. No new dissociation channel is expected to open. The additional translational energy that would be released is at best offset by the one quantum of stretch in its influence on the predissociation rate. It is therefore not surprising that we do not see any sign of predissociation for the three van der Waals bands of $C_6H_6\cdot Ar$ described here. For the s^2 level or levels with slightly higher energy, there might already be enough energy available and the new channel to the 16^1 level could open. Since the translation energy would then be small, a fast predissociation rate could well result. This might be why we are unable to observe these van der Waals states despite very careful search. The spectra shown in Figs. 1 and 2 and others recorded by us have a signal to noise ratio high enough to allow the observation of bands at least a factor of 100 weaker than the band at $+62.9\ \mathrm{cm}^{-1}$. The next higher van der Waals levels should not have Franck–Condon factors decreased by that much. Drastically increased intramolecular or intermolecular vibrational energy might, on the other hand, lead again to less favorable conditions for predissociation and consequently to highly stable states with energy far beyond the binding energy.

A mechanism known to produce large predissociation rates far above the ones predicted by Eq. (5) is the mixing of the optically excited (light) state of the cluster with dark background states through Fermi resonance.[58] The coupled dark states can have a dramatically faster predissociation rate. Even a small coupling matrix element can mix the light and the dark states very effectively if the zero order states are in near resonance. This idea is of particular interest for the systems under investigation in this work, as the band of $C_6H_6\cdot{}^{84}Kr$ at $+65.1\ \mathrm{cm}^{-1}$ and the band of $C_6D_6\cdot Ar$ at $+39.7\ \mathrm{cm}^{-1}$ show definitive signs of rotational perturbations. From our previous experience with the benzene monomer,[52,61,62] a possible assignment of these perturbations is either to weak anharmonic resonances with detuning of the coupled pairs of rovibronic levels due to differing rotational level structure or to Coriolis coupling with rotationally dependent coupling matrix elements. To explain the rotational selectivity of the coupling, the dark states have to be S_1 levels. Triplet levels cannot be responsible due to the large S_1-T_1 energy difference in benzene and the consequent statistical limit ISC process.[53]

Previous experimental investigations aimed at understanding the interplay between IVR and predissociation have concentrated on the analysis of single vibronic level fluorescence spectra.[1,13,60,63] Owing to the difference in binding energy between the S_0 and the S_1 state, the emission spectrum of a given state in the cluster is shifted from the one of the same state in the parent monomer. As a consequence, features in the spectrum often can be assigned uniquely to either the cluster or the monomer fragment of the predissociation. The quantitative analysis of the intensities allows the determination of the predissociation rate relative to the known fluorescence lifetime. In a similar fashion, a possible IVR process in the cluster (or mixing of levels) can be observed through altered emission patterns. Time-resolved emission[64] or time-resolved two-photon ionization[4] can render even more detailed information.

In the rotationally resolved spectra IVR is evidenced by perturbations of the otherwise regular rotational structure or by large differences in the effective rotational constants. This has been analyzed for the benzene monomer in great detail.[52,61,62] Only very strong anharmonic resonances will lead to homogeneous shifts of the whole band. However, such a strong coupling is not typical for mixing of the intramolecular modes with the van der Waals modes. Rapid dissociation of individual rovibronic states will result, on the other hand, in a broadening of lines and their eventual disappearance from the sub-Doppler spectrum. This situation is quite similar to the nonradiative decay of ''channel three'' benzene (for a review see Ref. 65).

For IVR to be effective, the molecule must have a large density of vibronic levels at the excess energy investigated. Typically, this requires an excess energy of $\sim 1500\ \mathrm{cm}^{-1}$ in small and rigid organic molecules. In clusters, however, there is an extra density of states originating from the added vibrational degrees of freedom. The possibility exists to compensate for the energy and symmetry mismatch between two intramolecular vibrational levels by addition of a suitable van der Waals level to the lower state. The benzene–Ar cluster has roughly the same vibrational level structure as that of the bare molecule (Table VII). Out-of-plane modes are known to cause slight shifts of levels;[1,4,13,34,66] all of the low lying levels in Table VII except ν_6 are out-of-plane modes. However, this should not influence the qualitative picture. We are concerned with possible coupling to either the 6^1 state or a van der Waals level built onto 6^1 with the same E_2 vibrational symmetry.

The possible couplings to a combination level $|\mathrm{vib,vdW}\rangle$ are governed by symmetry according to the selection rule

$$\Gamma_{\nu_6}\otimes\Gamma_{\mathrm{vib}}\otimes\Gamma_{\mathrm{vdw}}\otimes\Gamma_{\mathrm{coupling}}\supset A_1, \tag{8}$$

where $\Gamma_{\mathrm{coupling}}$ is A_1 for anharmonic, A_2 for parallel Coriolis, and E_1 for perpendicular Coriolis coupling. The results are shown in Table VIII for all possible cases of Γ_{vib} and both anharmonic and Coriolis coupling. It is seen that for the e_1 and e_2 vibrational states all symmetries of van der Waals states may participate. Since the low energy vibrational

TABLE VIII. Symmetry Γ_{vdW} of the van der Waals state needed to allow coupling of a combination state (intramolecular and intermolecular) with symmetry $\Gamma_{vib}\otimes\Gamma_{vdW}$ to the 6^1 state in benzene–rare gas clusters via anharmonic and parallel or perpendicular Coriolis coupling.

	Γ_{vdW} needed for coupling	
Vibrational symmetry Γ_{vib}	Anharmonic Parallel Coriolis	Perpendicular Coriolis
A_1,A_2	E_2	B_1,B_2,E_1
B_1,B_2	E_1	A_1,A_2,E_2
E_1	B_1,B_2,E_1	A_1,A_2,E_2
E_2	A_1,A_2,E_2	B_1,B_2,E_1

states are nearly all degenerate (cf. Table VII), we can conclude that nearly the full additional density of states introduced by the van der Waals degrees of freedom can contribute to the coupling and eventual intramolecular vibrational energy redistribution. The particular influence of a given level might, however, still be small since these will in general be governed by higher order couplings with very small coupling matrix elements. If this is the case, the observed spectrum will be unperturbed.

As an illustrative example, let us look at the possible coupling routes involving the $+65.1$ cm^{-1} level in $C_6H_6\cdot{}^{84}Kr$. The listing of intramolecular levels given in Table VII shows that the 10^1 level is quite close. Even without additional van der Waals excitation, there could be low-order perpendicular Coriolis coupling. Coupling to the 11^1 state would require about 70 cm^{-1} energy in the van der Waals state and an e_2 symmetry for anharmonic or parallel Coriolis coupling, or a b_1, b_2 or e_1 symmetry for perpendicular Coriolis coupling. The calculations of Brupbacher *et al.*[55] suggest that the $b^2(l=2)$ state might qualify for the former possibility and the s^1b^1 state for the latter. As we go to even lower lying states, we can expect even more possibilities. However, the necessary changes of vibrational quanta, i.e., the order of the coupling mechanism, will simultaneously increase.

Similar coupling routes also can be found for the state of $C_6D_6\cdot$Ar at $+39.7$ cm^{-1}. We conclude that the observed perturbations are indeed understandable within the model outlined. Whether couplings are active for a given state of a complex in the low energy range discussed here will depend strongly on accidental resonances. These can be varied by substitution of a different rare gas or isotopic substitution. Which particular coupling will be active in a given situation cannot be determined from symmetry considerations alone, at least with the present precision in the determination of both intramolecular and intermolecular frequencies. However, since only a few of the van der Waals bands are perturbed, apparently only a small fraction of the states can participate in IVR.

V. SUMMARY

We have described the rotationally resolved electronic spectra of eight van der Waals bands built onto the $6_0^1(S_1\leftarrow S_0)$ transition of benzene–rare gas clusters. Two bands of $C_6H_6\cdot{}^{84}Kr$ and the two higher energy ones of $C_6H_6\cdot$Ar and $C_6D_6\cdot$Ar were successfully interpreted as perpendicular transitions leading to combination states involving the intramolecular 6^1 state and van der Waals levels of A_1 symmetry. Only the lowest bands in $C_6H_6\cdot$Ar and $C_6D_6\cdot$Ar are found to neither display a simple perpendicular rotational structure nor a simple parallel one. The possible vibronic assignment of the van der Waals bands can be narrowed to two schemes by these observations and hinges now on the analysis of the two remaining bands. This will be described in the accompanying paper.[42]

The observation of sharp rovibronic lines in all the spectra is proof of the extremely low predissociation rate of the states that are to the best of our knowledge well above the dissociation limit. The additional excitation of van der Waals vibrations does not seem to increase the predissociation rate strongly. Rotational perturbations found in two of the reported bands are interpreted as coupling to dark combination states of intramolecular and intermolecular vibrational excitation. These couplings are the origin of IVR in a time dependent picture and possibly lead to increased dissociation rates.

ACKNOWLEDGMENTS

The authors wish to thank Professor Ad van der Avoird for valuable discussions. Financial support from the Deutsche Forschungsgemeinschaft is gratefully acknowledged.

[1] D. V. Brumbaugh, J. E. Kenny, and D. H. Levy, J. Chem. Phys. **78**, 3415 (1983).
[2] J. A. Menapace and E. R. Bernstein, J. Phys. Chem. **91**, 2533 (1987).
[3] P. M. Weber, J. T. Buontempo, F. Novak, and S. A. Rice, J. Chem. Phys. **88**, 6082 (1988).
[4] B. A. Jacobson, S. Humphrey, and S. A. Rice, J. Chem. Phys. **89**, 5624 (1988).
[5] E. J. Bieske, M. W. Rainbird, I. M. Atkinson, and A. E. W. Knight, J. Chem. Phys. **91**, 752 (1989).
[6] E. J. Bieske, M. W. Rainbird, and A. E. W. Knight, J. Chem. Phys. **94**, 7019 (1991).
[7] M. Mons, J. Le Calvé, F. Piuzzi, and I. Dimicoli, J. Chem. Phys. **92**, 2155 (1990).
[8] M. Mons and J. Le Calvé, Chem. Phys. **146**, 195 (1990).
[9] M. Schmidt, M. Mons, and J. Le Calvé, Z. Phys. D **17**, 153 (1990).
[10] P. Hermine, P. Parneix, B. Coutant, F. G. Amar, and Ph. Bréchignac, Z. Phys. D **22**, 529 (1992).
[11] P. Parneix, N. Halberstadt, Ph. Bréchignac, F. G. Amar, A. van der Avoird, and J. W. I. van Bladel, J. Chem. Phys. **98**, 2709 (1993).
[12] B. B. Champagne, D. F. Plusquellic, J. F. Pfanstiel, D. W. Pratt, W. M. van Herpen, and W. L. Meerts, Chem. Phys. **156**, 251 (1991).
[13] M.-C. Su, H.-K. O, and C. S. Parmenter, Chem. Phys. **156**, 261 (1991).
[14] S. Yan and L. H. Spangler, J. Phys. Chem. **95**, 3915 (1991).
[15] D. Consalvo, A. van der Avoird, S. Piccirillo, M. Coreno, A. Giardini-Guidoni, A. Mele, and M. Snels, J. Chem. Phys. **99**, 8398 (1993).
[16] V. Stert, W. Radloff, H.-H. Ritze, and Th. Freudenberg, Chem. Phys. Lett. **204**, 287 (1993).
[17] M. Mandziuk, Z. Bačić, T. Droz, and S. Leutwyler, J. Chem. Phys. **100**, 52 (1994).
[18] M. Takayanagi and I. Hanazaki, Spectrochim. Acta **50A**, 1435 (1994).
[19] P. Hobza, H. L. Selzle, and E. W. Schlag, J. Chem. Phys. **95**, 391 (1991).
[20] P. Hobza, O. Bludský, H. L. Selzle, and E. W. Schlag J. Chem. Phys. **97**, 335 (1992).
[21] Th. Brupbacher, H. P. Lüthi, and A. Bauder, Chem. Phys. Lett. **195**, 482 (1992).
[22] H.-Y. Kim and M. W. Cole, J. Chem. Phys. **90**, 6055 (1989).
[23] G. Brocks and T. Huygen, J. Chem. Phys. **85**, 3411 (1986).

[24] A. R. Tiller and D. C. Clary, Chem. Phys. **139**, 67 (1989).
[25] O. Bludský, V. Špirko, V. Hrouda, and P. Hobza, Chem. Phys. Lett. **196**, 410 (1992).
[26] A. van der Avoird, J. Chem. Phys. **98**, 5327 (1993).
[27] M. Mandziuk and Z. Bačić, J. Chem. Phys. **98**, 7165 (1993).
[28] J. Faeder, J. Chem. Phys. **99**, 7664 (1993).
[29] C. A. Haynam, D. V. Brumbaugh, and D. H. Levy, J. Chem. Phys. **79**, 1581 (1983); **80**, 2256 (1984).
[30] D. F. Plusquellic, X.-Q. Tan, and D. W. Pratt, J. Chem. Phys. **96**, 8026 (1992); A. Held and D. W. Pratt, J. Am. Chem. Soc. **115**, 9708 (1993).
[31] G. Meijer, G. Berden, W. L. Meerts, H. E. Hunziker, M. S. de Vries, and H. R. Wendt, Chem. Phys. **163**, 209 (1992); G. Berden and W. L. Meerts, Chem. Phys. Lett. **224**, 405 (1994).
[32] Th. Weber, A. von Bargen, E. Riedle, and H. J. Neusser, J. Chem. Phys. **92**, 90 (1990).
[33] Th. Weber, E. Riedle, H. J. Neusser, and E. W. Schlag, Chem. Phys. Lett. **183**, 77 (1991).
[34] Th. Weber, E. Riedle, and H. J. Neusser, Z. Phys. D **20**, 43 (1991).
[35] Th. Weber, E. Riedle, H. J. Neusser, and E. W. Schlag, J. Mol. Struct. **249**, 69 (1991).
[36] Th. Weber and H. J. Neusser, J. Chem. Phys. **94**, 7689 (1991).
[37] H. J. Neusser, R. Sussmann, A. M. Smith, E. Riedle, and Th. Weber, Ber. Bunsenges. Phys. Chem. **96**, 1252 (1992).
[38] R. Sussmann and H. J. Neusser, Chem. Phys. Lett. **221**, 46 (1994); R. Sussmann, U. Zitt, and H. J. Neusser, J. Chem. Phys. **101**, 9257 (1994).
[39] R. Sussmann, R. Neuhauser, and H. J. Neusser, Can. J. Phys. **72**, 1179 (1994); R. Sussmann, R. Neuhauser, and H. J. Neusser, Chem. Phys. Lett. **229**, 13 (1994).
[40] H. J. Neusser and R. Sussmann, in *Jet Spectroscopy and Molecular Dynamics*, edited by J. M. Hollas and D. Phillips (Chapman and Hall, London, 1995).
[41] R. Sussmann and H. J. Neusser, J. Chem. Phys. **102**, 3055 (1995).
[42] E. Riedle and A. van der Avoird, J. Chem. Phys. **104**, 882 (1996).
[43] E. Riedle, Th. Knittel, Th. Weber, and H. J. Neusser, J. Chem. Phys. **91**, 4555 (1989).
[44] R. Weinkauf, K. Walter, C. Weikhardt, U. Boesl, and E. W. Schlag, Z. Naturforsch. **44a**, 1219 (1989).
[45] J. H. Callomon, T. M. Dunn, and I. M. Mills, Philos. Trans. R. Soc. London, Ser. A **259**, 499 (1966); G. H. Atkinson and C. S. Parmenter, J. Mol. Spectrosc. **73**, 20, 31, 52 (1978).
[46] N. Gonohe, N. Suzuki, H. Abe, N. Mikami, and M. Ito, Chem. Phys. Lett **94**, 549 (1983).
[47] A. W. Garrett, R. N. Pribble, A. J. Gotch, and T. S. Zwier, in *Advances in Multiphoton Processes and Spectroscopy*, edited by S. H. Lin, A. A. Villaeys, and Y. Fujimura (World Scientific, Singapore, 1994), Vol. 8, Part 2, p. 129.
[48] Th. Brupbacher and A. Bauder, Chem. Phys. Lett. **173**, 435 (1990).
[49] T. D. Klots, T. Emilsson, and H. S. Gutowsky, J. Chem. Phys. **97**, 5335 (1992).
[50] J. Plíva and A. S. Pine, J. Mol. Spectrosc. **93**, 209 (1982).
[51] J. Plíva, A. Valentin, J. Chazelas, and L. Henry, J. Mol. Spectrosc. **134**, 220 (1989).
[52] E. Riedle, Th. Weber, U. Schubert, H. J. Neusser, and E. W. Schlag, J. Chem. Phys. **93**, 967 (1990).
[53] For a review, see C. S. Parmenter, Adv. Chem. Phys. **22**, 365 (1972).
[54] Th. Weber, dissertation, Technische Universität München, 1991.
[55] Th. Brupbacher, J. Makarewicz, and A. Bauder, J. Chem. Phys. **101**, 9736 (1994).
[56] P. M. Maxton, M. W. Schaeffer, S. M. Ohline, W. Kim, V. A. Venturo, and P. M. Felker, J. Chem. Phys. **101**, 8391 (1995).
[57] H. Krause and H. J. Neusser, J. Chem. Phys. **97**, 5923 (1992); **99**, 6278 (1993).
[58] G. E. Ewing, J. Phys. Chem. **90**, 1790 (1986); **91**, 4662 (1987), and references therein.
[59] K. W. Butz, D. L. Catlett, Jr., G. E. Ewing, D. Krajnovich, and C. S. Parmenter, J. Phys. Chem. **90**, 3533 (1986).
[60] T. A. Stephenson and S. A. Rice, J. Chem. Phys. **81**, 1083 (1984).
[61] E. Riedle and J. Plíva, Chem. Phys. **152**, 375 (1991).
[62] H. Sieber, E. Riedle, and H. J. Neusser, J. Chem. Phys. **89**, 4620 (1988).
[63] J. J. F. Ramaekers, H. K. van Dijk, J. Langelaar, and R. P. H. Rettschnick, Faraday. Discuss. Chem. Soc. **75**, 183 (1983).
[64] D. H. Semmes, J. S. Baskin, and A. H. Zewail, J. Chem. Phys. **92**, 3359 (1990).
[65] E. Riedle, H. J. Neusser, and E. W. Schlag, Philos. Trans. R. Soc. London, Ser. A **332**, 189 (1990).
[66] B. Coutant and P. Brechignac, J. Chem. Phys. **100**, 7087 (1994).